Scientific Research Publishing

Open Journal of Civil Engineering, 2024, 14, 155-167
https://www.scirp.org/journal/ojce
ISSN Online: 2164-3172
ISSN Print: 2164-3164

Experimental Study of the Anti-Corrosion Performance of Montmorillonite K-10 on Rebar in HCl Environment: Application in Mortar for the Rehabilitation of Reinforced Concrete Degraded by Corrosion

Malang Bodian[1], Mariétou Barro Diop-Fall[1], Dame Keinde[2], El-Hadji Dieye[2], Modou Gningue Diop[1], Modou Fall[1]

[1]Laboratoire de Chimie Physique Organique et d'Analyse Environnementales (LCPOAE), Département de Chimie, Univ Cheikh Anta Diop de Dakar, Dakar, Senegal
[2]Laboratoire de Matériaux de Génie Civil (LMGC), Ecole Supérieure Polytechnique de Dakar, Univ Cheikh Anta Diop, Dakar, Sénégal

Email: bodianthomas@gmail.com, maribarrodiop@gmail.com, dkeinde85@yahoo.fr, elhadjidieye91@gmail.com, modougninguediop@gmail.com, modou.fall@ucad.edu.sn

How to cite this paper: Bodian, M., Diop-Fall, M.B., Keinde, D., Dieye, E., Diop, M.G. and Fall, M. (2024) Experimental Study of the Anti-Corrosion Performance of Montmorillonite K-10 on Rebar in HCl Environment: Application in Mortar for the Rehabilitation of Reinforced Concrete Degraded by Corrosion. *Open Journal of Civil Engineering*, **14**, 155-167.
https://doi.org/10.4236/ojce.2024.142008

Received: March 27, 2024
Accepted: June 22, 2024
Published: June 25, 2024

Abstract

This work first investigates the corrosion-inhibiting behavior of montmorillonite K-10 on reinforcing steel. The corrosion-inhibiting power of the clay (Montmorillonite) is determined in a medium HCl (C = 1N) using free corrosion potential monitoring, Tafel potentiodynamic polarization curves and electrochemical impedance spectroscopy. The results of this study showed a satisfactory corrosion-inhibiting efficiency of around 72.665% for the optimum content of 1%. This is due to the presence of a stable oxide layer that protects the metal against corrosion. To validate the concept of montmorillonite as a corrosion inhibitor in repair mortar, we now turn to the influence of montmorillonite on the mechanical properties of mortars in the hardened state. In this part, montmorillonite K-10 is added to the mortar by partial substitution of the cement by 5% and 10% of the cement mass. The aim of this study is to ensure that the addition of this clay to the mortar composition will not have a negative effect on its compressive and flexural strengths. The results of the compression and flexural tests showed that the presence of montmorillonite in the mortar improved flexural and compressive strengths

for the different compositions studied.

Keywords

Clay, Reinforced Concrete, Corrosion, Inhibitor, Rehabilitation, Electrochemical Methods

1. Introduction

The repair and rehabilitation of reinforced concrete structures are a fast-growing sector in Senegal. Indeed, a large proportion of reinforced concrete structures located by the sea require maintenance and repair work, given their state of deterioration. Corrosion of the reinforcement in concrete is considered to be one of the main causes of the deterioration of these structures. Steel in concrete is normally in a passive, non-corrosive state. However, these passive non-corrosive conditions are not always achieved in practice, due to the corrosion of the reinforcing bars and the heterogeneity of the concrete-reinforcement matrix [1]. Reinforcing bar corrosion is a major universal problem, with physical consequences such as a reduction in the ultimate strength of the steel-concrete bond. It is also the key factor affecting the durability and safety of reinforced concrete buildings and structures [2]. Corrosion is the leading cause of deterioration in reinforced concrete structures, accounting for 47% of all types of damage according to a Europe-wide survey of managers of concrete structures [3]. This problem represents a major technological and economic challenge, prompting researchers to find fast, effective solutions to extend the service life of structures, ensure user safety and optimize maintenance and repair costs [4]. There are numerous repair methods for corroded reinforced concrete structures, including mortar repair. However, few studies have been carried out on the durability of repair mortars. This is why we aim to contribute to the development of repair mortars capable of slowing down the progression of corrosion for a more effective and durable repair.

The aim of this work is firstly to study the anti-corrosion performance of montmorillonite K-10 on reinforcing steel, secondly, to evaluate the effect of montmorillonite on the mechanical strength of mortar, with a view to its application in the repair of reinforced concrete structures.

2. Condition and Experimental Methods

2.1. Electrochemical Methods for Assessing Corrosion and Inhibition Efficiency

In the electrochemical experiments, clay is introduced into the solution from HCl à. The clay content varies from 0.5% to 2% of the solution mass. To avoid deposition of the K-10 CMM at the bottom of the beaker, a bar magnet is used as a stirrer throughout the experiment.

The working electrode used in this study is a 10 mm diameter HA FeE500-3 hardened (high adhesion) rebar, used in the construction of reinforced concrete structures. It consists of 98% iron, a carbon content of 0.02 to 0.2 by mass and other chemical elements such as chromium (Cr), nickel (Ni), molybdenum (Mo) and manganese (Mn).

Steel bar preparation begins by removing the oxide layer with a wire brush. The steel surface in contact with the electrolytic solution of HCl electrolytic solution is then isolated from the rest of the bar by an "Epoxy Steel" type resin (see Figure 1). Prior to all measurements, the exposed parts of the steel bars (immersed in the HCl solution) were polished with 350 µm and then 250 µm respectively, to remove oxide films and the various deposits forming on the surface of these steels, then rinsed with distilled water and air-dried.

The experimental set-up used for electrochemical testing comprises a portable MetrohmDropsensµStat-i 400 s potentiostat/galvanostat. Controlled by DropView 8400 software, it is coupled to an electrochemical cell comprising a set of three electrodes immersed in a beaker (see Figure 2). The sample is the working electrode, the counter-electrode is a steel grid, and the reference electrode for all electrochemical measurements is Ag/AgCl (+197 mV/ENH at room temperature).

Electrochemical methods provide interesting insights into corrosion potential, corrosion rate, inhibitor mechanism of action and charge transfer resistance. These methods include open-circuit corrosion potential monitoring, potentiodynamic polarization and electrochemical impedance spectroscopy:

Steel corrosion was studied by monitoring the corrosion free potential during a 2 h (3600 s) immersion period.

Tafel's potentiodynamic polarization technique is performed by sweeping the potential between −0.25 V and 0.25 V relative to the OCP (Open Circuit Potential) at a speed of 0.1 mV/s.

Electrochemical impedance measurements are recorded after stabilization of the corrosion free potential with an amplitude of 50 mV. Potential sweeps are performed at variable frequencies in the 100 Hz - 10 mHz with 5 points per decade.

The electrical circuit proposed in this study for simulating impedance diagrams is shown in Figure 3.

For the equivalent electrical diagram, the interface behaves dynamically like a capacitor called a double-layer capacitor $C_{dc} = C$. The diagram also includes a charge transfer resistor $R_{cR} = R$ at the low-frequency limit. This electrical or electrochemical double layer is described by the Gouy-Chapman-Stern model.

EI inhibitory efficacy (%) is calculated as follows:

$$EI(\%) = \frac{R'_{tc} - R_{tc}}{R'_{tc}} \times 100 \quad (1)$$

With R'_{tc} and R_{tc} are the charge transfer resistance values in the presence and absence of the inhibitor under study, respectively.

Figure 1. The working electrode.

Figure 2. The MetrohmDropsens instrument and installation [5].

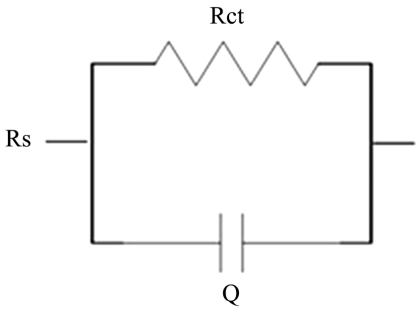

Figure 3. Equivalent circuit used to model impedance spectra.

2.2. Methods for Assessing the Mechanical Behavior of Inhibitor-Based Mortars

The mortar used in our work is formulated with SOCOCIM 42.5R cement, dune sand and tap water. Mortar composition isdetailed in Table 1.

Montmorillonite is added to the mortar as a cement substitute at contents of 5% and 10% of the cement mass (see Table 2). Its chemical composition is presented in Table 3. The aim of this study is to analyze the effect of montmorillonite on compressive strengths, with a view to testing it as a repair mortar for corrosion-damaged structures.

Montmorillonite-based mortars were produced under the same conditions (quantities) as the reference mortar.

Each prepared composition was cast and compacted in three (3) steel moulds of size 4 × 4 × 16 cm^3 well-oiled with a brush for easy stripping in accordance with EN196-1. The molds were demolded after 24 hours in a damp room, then stored in a basin of water for a cure of 14 days and 28 days (to allow the cement and clay to continue reacting). At different times of 14 and 28 days under water, three specimen samples were taken out and subjected to mechanical tests (flexural and compressive strengths).

The bending test is carried out on prismatic mortar specimens in accordance with NF EN 196-1 using a semi-automatic press (see Figure 4) with a bending capacity of 10 kN. Tests are carried out at speeds of 11.250 kN/s. For each composition, three (3) specimens measuring 40 × 40 × 160 cm^3 are tested at 14 days and 28 days of curing.

Table 1. Studymortar formulation.

Materials	Dosage (kg/m^3)
Cement II/B-M 32.5 R	507
Sand	1521
Water	253
E/C	0.5
C/S	3

Table 2. Formulation of montmorillonite mortar.

Materials	Dosage (kg/m^3)		
	Reference	5% MMT K-10	10% MMT K-10
Cement	507.000	482.918	456.300
Sand	1521.000	1521.000	1521.000
Water	253.000	253.000	253.000
MMT K-10	0.000	24.146	45.630
E/C		0.500	

Table 3. Chemical composition of Montmorillonite K-10 clay [6].

Name	Chemical elements (%)							
	SiO_2	Al_2O_3	CaO	MgO	Na_2O	K_2O	Fe_2O_3	H_2SO_4
MMT K-10	73	14	0.2	1.1	0.6	1.9	2.7	-

Flexural strength of specimens 4 × 4 × 16 cm^3 in MPa is given by the formula:

$$f_f\left(MPa\right)=\frac{1.5\times F_f\times L}{b^3}=\frac{1.5\times F_f\times 100}{40^3}=0.00234375\times F_f\left(N\right) \quad (2)$$

With:

- f_f : bending strength in MPa.
- b: specimen thickness in mm.
- L: is the distance between two supports in mm.
- F_f : Load appied to the middle of the prism at break in MPa.

Compressive strength was measured on half-test specimens obtained after flexural fracture using the same machine with an appropriate compression fixture (Figure 5). The loading speed was the same as for the flexural strength study (11.250 kN/s).

The compressive strength $f_c\left(MPa\right)$ is given by the formula:

$$f_c\left(MPa\right)=\frac{F_c}{A}=\frac{F_c\left(N\right)}{1600\left(mm^2\right)} \quad (3)$$

With:

- F_c : the maximum force reached during the test (N);
- A: is the cross-sectional area of the specimen (mm^2).

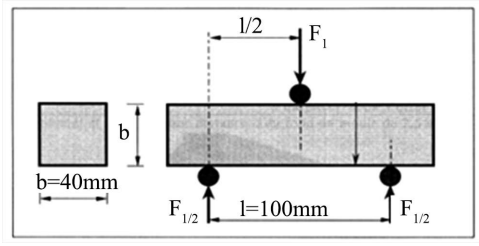

Figure 4. Bending test.

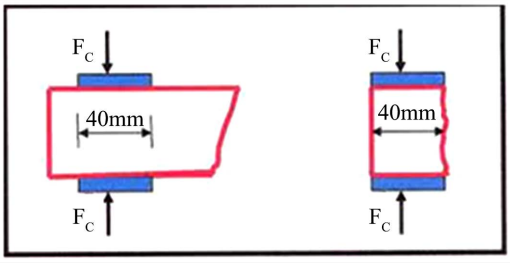

Figure 5. Compression test.

Mortar strength at the age in question is obtained by calculating the average of the 6 half-prisms. If one of the 6 results differs by ±10% from this average, it is discarded and the average is then calculated from the 5 remaining results. If one of the 5 results again deviates by ±10% from this new average, the series of 6 measurements is discarded. In this case, the reasons for the discrepancy should be investigated: mixing, placement, storage, etc. [7].

3. Results and Discussions

3.1. Study of the Inhibitory Efficacy of Montmorillonite K-10

In this section, we analyze the corrosion inhibiting power of K-10 montmorillinite on concrete iron using electrochemical methods such as open-circuit corrosion potential (OCP) monitoring, potentiodynamic polarization and electrochemical impedance spectroscopy.

3.1.1. Open Circuit Corrosion Potential (OCP) Monitoring

Figure 6 shows the corrosion potential versus ECS of the steel electrode as a function of time (2 h immersion) in a solution of HCl 1 N solution in the absence and presence of montmorillonite k-10 (MM K-10) at room temperature. The corrosion potential values recorded after 2 h are shown in Table 4.

It can be seen from Figure 6 that the corrosion potential of the reference shifts rapidly with time, reaching a stationary value at around 30 min, and its curve is below the other curves with a variation of around −0.509 to −0.498 V/ECS.

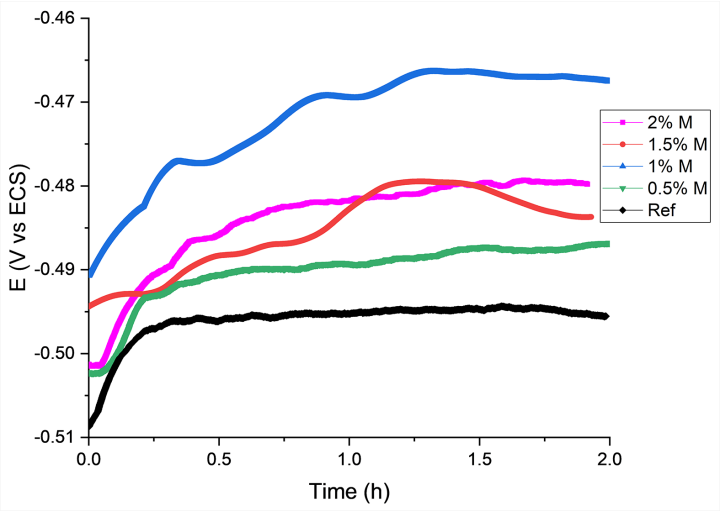

Figure 6. Monitoring corrosion potential as a function of immersion time for steel in HCl.

Table 4. Potential values measured in an OCP.

Sample	Ref	0.5% M	1% M	1.5%M	2%M
E (V/ECS)	−0.498	−0.489	−0.467	−0.487	−0.486

In the presence of the K-10 CMM, compared with the reference, the corrosion potential improves, reaching a quasi-stationary state after 2 hours of immersion (see Figure 6). This evolution towards anodic values in the presence of clay could be explained by the formation of a more or less stable corrosion layer protecting the iron [8].

Figure 6 also shows that the corrosion potential curves in the presence of clay show disturbances reflecting interaction between clay and chloride ions [9].

Looking at Table 4, we can see that the corrosion potential recorded after 2 hours is more positive than in the presence of clay. The values are −0.498 for the reference, −0.489 for 0.5%, −0.467 for 1%, −0.487 for 1.5% and −0.486 for 2%.

This enhancement of corrosion potential in the presence of clay shows the clay's corrosion-inhibiting effect. This inhibition could be explained by the presence of a protective oxide layer on the steel surface.

3.1.2. Potentiodynamic Polarization

Potentiodynamic polarization curves performed at different concentrations in the presence or absence of MMK-10 after 2 hours immersion at room temperature in a solution of HCl 1 N solution are shown in Figure 7. The electrochemical parameters derived from these curves are presented in Table 5.

Figure 7 shows a shift in corrosion potential towards anodic values after each addition of clay.

We also observe that the presence of clay in the HCl solution did not affect cathodic reactions. On the other hand, the current density of the anodic branches decreased at concentrations of 0.5% and 1%, reflecting a change in the oxidation reaction of the steel, with the formation of a stable corrosion film protecting the metal.

From these findings, we can say that the evolution of corrosion potential towards anodic values shows that MM K-10 behaves as an anodic inhibitor with the formation of a passivation layer.

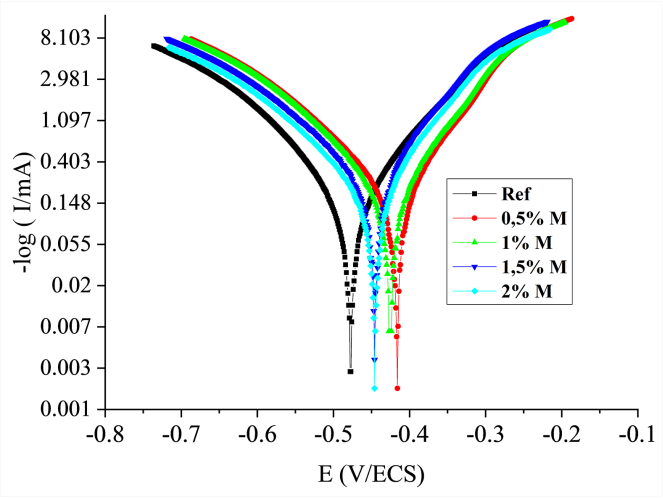

Figure 7. Polarization curves for steel after 2 h immersion in a HCl 1 N.

Table 5. Parameter values obtained when measuring polarization in different concentrations of montmorillonite K-10.

	Rp ($k\Omega \cdot cm^2$)	$\mathbf{E_{corr}}$ (V/ECS)	$\mathbf{i_{corr}}$ ($\mu A/cm^2$)	βa (V/dec.)	βc (V/dec.)	$\mathbf{V_{corr}}$ (mm/year)	EI (%)
Ref	0.131	−0.492	211.657	0.134	0.122	2.591	-
0.5% M	0.165	−0.419	114.898	0.099	0.078	1.337	45.715
1% M	0.235	−0.426	57.856	0.066	0.059	0.673	72.665
1.5% M	0.159	−0.446	133.309	0.114	0.085	1.552	37.016
2% M	0.169	−0.446	123.846	0.117	0.082	1.442	41.487

Table 5 shows that, in the absence of the MMK-10, the corrosion rate is of the order of 2.591 mm/year which is proportional to the corrosion current density 211.657 $\mu A/cm^2$ and a polarization resistance of 0.131 $k\Omega \cdot cm^2$.

In the presence of the inhibitor, a decrease in current density and corrosion rate compared with the control was observed for each grade (Table 5). Conversely to the variation in current density and corrosion rate, all grades show an increase in polarization resistance compared with the control. However, the 1% montmorillonite K-10 content has the lowest current density (57.856 $\mu A/cm^2$) and the highest corrosion resistance (0.235 $k\Omega \cdot cm^2$). However, above 1% of the mass, the polarization resistance is lowered and the corrosion rate increased (current densities). In addition, better corrosion inhibition was recorded for the 1% MM K-10 content, with an inhibitory efficiency of 72.665%.

On the basis of these observations, we can conclude that montmorillonite K-10 has appreciable inhibiting power at an optimum content of 1%.

3.1.3. Electrochemical Impedance Spectroscopy

Impedance diagrams were also plotted at corrosion potential (E_{corr} = reference V/ECS) to validate the conclusions drawn from the anodic polarization curves in Figure 8. The impedance diagrams recorded after 2 h of open-circuit corrosion potential monitoring are reproduced in Figure 8. All electrochemical parameters resulting from the evaluation of these impedance spectra are reported in Table 6.

In the Nyquist plane (Figure 8), the impedance diagrams of the specimens have the same profile, with loops in the form of semicircles of distinct diameters. The diameter of the arcs corresponding to electrochemical reactions is greater in the presence of clay. However, the 1% inhibitor content has the largest diameter. The evolution of capacitive loops by the addition of MMK-10 defines a resistance to the charge transfer reaction by the formation of a passive-type protective oxide layer on the metal surface. At the same time, the reduction in diameters beyond 1% shows that the protective film has become less effective. This resistance to the charge transfer reaction is all the greater when the clay content equals 1%.

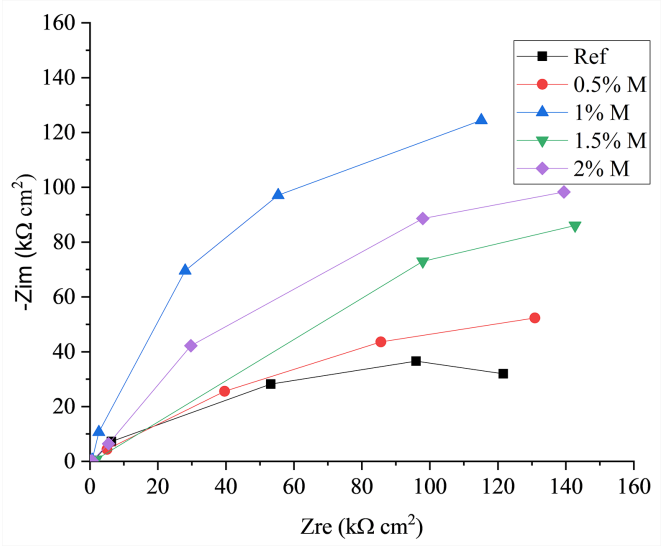

Figure 8. Nyquist impedance diagrams of steel in solution HCl 1 N solution at different inhibitor mass concentrations.

Table 6. Parameters for measuring electrochemical impedance spectra in different mass concentrations of montmorillonite K-10.

	R_s (kΩ·cm²)	Q (nF·cm⁻²)	n	R_{tc} (kΩ·cm²)	EI (%)
Ref	0.883	0.094	0.999	118.292	-
0.5% M	1.519	0.423	0.993	299.987	60.568
1% M	4.733	0.576	1.000	435.753	72.853
1.5% M	3.387	0.445	0.989	187.895	37.044
2% M	4.975	0.452	1.000	207.264	42. 927

Table 6 shows that the CPE (Constant Phase Element) or Q is lower in the presence of the MMK-10. At the same time, the load transfer resistance is greater in the presence of the MMK-10. The values of the empirical coefficient n are close to 1. In these cases, the CPE can be assimilated to a pure capacitance, the deviation from unity reflecting surface inhomogeneities [10]. The decrease in Q in the presence of montmorillonite reflects the formation of an oxide film at the steel-solution interface.

However, the 1% montmorillonite content has the highest charge transfer resistance (435.753 kΩ·cm²) and the highest inhibitory efficiency (72.853%). This illustrates that the film formed at this content (1%) is stable and protects the metal. Above 1%, the passive film is unstable and porous.

3.2. Effect of Montmorillonite K-10 on Mortar Mechanical Strength

To confirm the application of montmorillonite in repair mortar, we tested in this section the influence of clay on the mortar's mechanical properties.

3.2.1. Flexural Strength

Figure 9 shows the force values exerted on the samples and the corresponding flexural strength at 14 and 28 days of curing.

Figure 9 shows that, for each given composition, the flexural strengths of repair mortars aged 14 days are lower than those aged 28 days. This reflects an advancement of the hydration reaction with mortar maturation age.

In addition, strength increases with increasing clay content. Flexural strengths of 3.6047 MPa and 4.4783 MPa respectively at 14 and 28 days of curing for the 10% composition. The control has minimum values of 1.6465 MPa and 3.112 MPa at 14 and 28 days respectively. It can be deduced from these findings that the presence of the clay-based inhibitor has a positive impact on the flexural strength of the mortars. This improvement in flexural strength could be explained by reactivity between the silica in MM K-10 and the cement hydrates [11]. As a result, MM K-10 guarantees the suitability and longevity of reinforced concrete.

3.2.2. Compressive Strength

Figure 10 shows the histogram illustrating the evolution of compressive strengths at 14 and 28 days of curing.

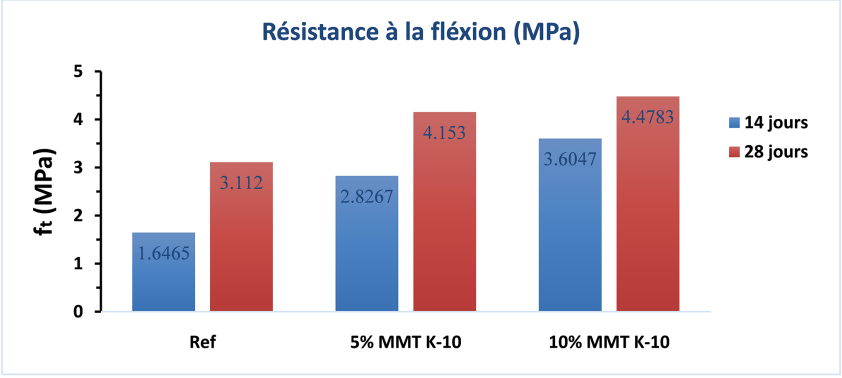

Figure 9. Bending strengths at 14 and 28 days of the three mortars studied.

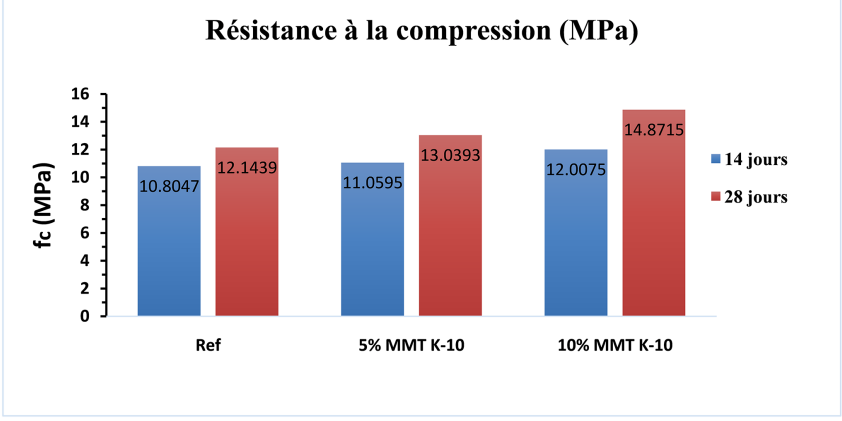

Figure 10. Compressive strengths at 14 and 28 days of the three mortars studied.

As in the case of flexural strengths, **Figure 10** shows that, for each given composition, the compressive strengths of 14-day-old repair mortars are lower than those of 28-day-old mortars. This confirms the advancement of the hydration reaction with mortar maturation age.

In the presence of montmorillonite, resistance increases with the clay content. Values of 10.8 for the control and 12 MPa for the 10% were noted at 14 days of ripening. At 28 days of curing, compressive strengths increased by 12.1 for the control and 15 MPa for the composition with 10% MM K-10. The 5% clay composition shows a value of 11 and 13 MPa respectively at 14 and 28 days. These results show that the presence of the clay inhibitor as an additive in the concrete mortar has a positive impact on compressive strength. This improvement in compressive strength could be explained by a strengthening of mortar porosity [11].

4. Conclusions

This work was carried out to contribute to the development of repair mortars capable of slowing down the progression of corrosion, for more effective and longer-lasting repairs. Firstly, the anti-corrosion performance of montmorillonite K-10 on reinforcing steel was studied. Secondly, this study assessed the effect of montmorillonite on the mechanical resistance of mortar, with a view to its application in the repair of reinforced concrete structures.

Experimental results from the study of the corrosion inhibiting power of montmorillonite on concrete reinforcing steel in the HCl carried out using electrochemical methods, show that the 1% montmorillonite content has the best inhibiting efficacy (72.853%). This is due to the formation of a montmorillonite-based film that protects the steel.

Mechanical tests carried out on clay-containing mortars using compression and flexural tests have shown that the presence of montmorillonite K-10 also improves a mortar's flexural and compressive strengths.

This work could also be continued with tests at montmorillonite contents below 5% and above 10%. In this study, we were unable to characterize the properties of the mortars in the fresh state. In the short term, it would be interesting to carry out tests on the setting time and Abrams cone slump of these mortars, in order to obtain information on the workability of this mortar.

In the long term, it would also be important to study the resistance to chloride penetration and carbonation of reinforced mortars based on montmorillonite K-10.

Conflicts of Interest

The authors declare no conflicts of interest regarding the publication of this paper.

References

[1] Angst, U.M., Geiker, M.R., Michel, A., Gehlen, C., Wong, H., Isgor, O.B., *et al.*

(2017) The Steel-Concrete Interface. *Materials and Structures*, **50**, 143. https://doi.org/10.1617/s11527-017-1010-1

[2] Khanzadeh Moradllo, M., Qiao, C., Ghantous, R.M., Zaw, M., Hall, H., Ley, M.T., *et al.* (2020) Quantifying the Freeze-Thaw Performance of Air-Entrained Concrete Using the Time to Reach Critical Saturation Modelling Approach. *Cement and Concrete Composites*, **106**, Article ID: 103479. https://doi.org/10.1016/j.cemconcomp.2019.103479

[3] Hubert, B. (2002) Approche des études géotechniques liées à la pathologie des ouvrages. *Géologues* (*Paris*), **132**, 97-106.

[4] Benzargoun, Messaouda et Touban, Nadjat. (2020) Etude de L'effet inhibiteur sur l'extrait de plante Calotropis Procera (Krnaka) la corrosion de L'acier X70 en milieu acide HCl 1M. Thèse de Doctorat. Université de Ghardaïa.

[5] Nagendrappa, G. (2002) Organic Synthesis Using Clay Catalysts. *Resonance*, **7**, 64-77. https://doi.org/10.1007/bf02836172

[6] Diallo, M.D., Diop, S.N., Diémé, M.M. and Diawara, C.K. (2020) Removal of Fluoride in Brackish Drinking Water from Senegal by Using KSF and K10 Montmorillonite Clays. *International Journal of Applied Chemistry*, **7**, 65-70. https://doi.org/10.14445/23939133/ijac-v7i3p112

[7] Rahim, O., Achoura, D., Benzerara, M. and Bascoulès-Perlot, C. (2021) Experimental Contribution to the Study of the Physic-Mechanical Behavior and Durability of High-Performance Concretes Based on Ternary Binder (Cement, Silica Fume and Granulated Blast Furnace Slag). *Frattura ed Integrità Strutturale*, **16**, 344-358. https://doi.org/10.3221/igf-esis.59.23

[8] Bodian, M. (2022) Étude par voies électrochimique, physique et mécanique des effets de la corrosion des armatures métalliques sur les performances de l'adhérence acier-béton. Thèse de cotutelle entre UCAD et INSA de Rennes.

[9] Garcés, P., Saura, P., Méndez, A., Zornoza, E. and Andrade, C. (2008) Effect of Nitrite in Corrosion of Reinforcing Steel in Neutral and Acid Solutions Simulating the Electrolytic Environments of Micropores of Concrete in the Propagation Period. *Corrosion Science*, **50**, 498-509. https://doi.org/10.1016/j.corsci.2007.08.016

[10] Tritthart, J. (2003) Transport of a Surface-Applied Corrosion Inhibitor in Cement Paste and Concrete. *Cement and Concrete Research*, **33**, 829-834. https://doi.org/10.1016/s0008-8846(02)01067-0

[11] Bodian, M., Keinde, D., Yade, I., Hannawi, K., Agbodjan, P.W., Fall, M. and Darquennes, A. (2022) Study of Attapulgite as an Additive in Reinforced Concrete by Substitution of Cement and Its Effects on the Durability Properties of Hardened Concrete. *Open Journal of Civil Engineering*, **12**, 301-319. https://doi.org/10.4236/ojce.2022.123018